Cell Reports, Volume *33*

Supplemental Information

A Systematic Protein Turnover Map

for Decoding Protein Degradation

Romain Christiano, Henning Arlt, Sonja Kabatnik, Niklas Mejhert, Zon Weng Lai, Robert V. Farese Jr., and Tobias C. Walther

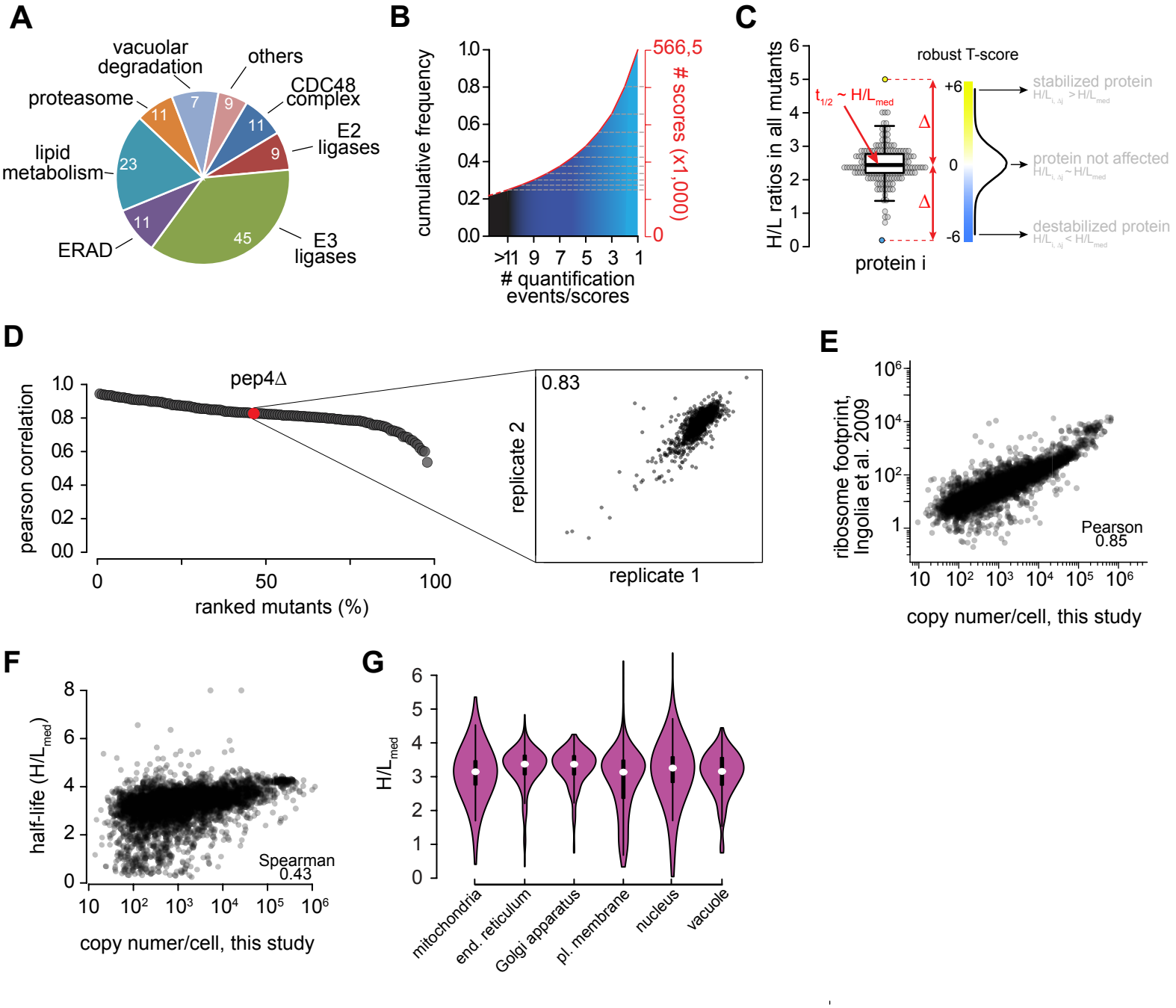

Suppl. Figure 1: Quality of Turnover Data, Related to Figure 1 (A) Pie chart of mutants included in the T-MAP categorized by biological function (described in Table S1). (B) Cumulative frequency of the number of scores (proteins quantified) in the T-MAP as a function of quantification events/score. (C) Scoring function for quantitative turnover analysis identifies destabilizing ($H/L_{i.\Delta j} < H/Lmed$), stabilizing ($H/L_{i.\Delta j} > H/L_{med}$) and neutral ($H/L_{i.\Delta j} \sim H/L_{med}$) effects of mutant Δj on protein *i*. (D) Reproducibility of turnover profiling between independent biological duplicates (coefficient of correlation) for each mutant in the screen. Inlay shows as an example the reproducibility between biological replicates of *pep4*Δ. (E) Correlation of protein abundance measurements determined in this study to ribosome footprint data from Ingolia et al., 2009 (Pearson correlation coefficient: 0.85). (F) Correlation between protein abundance and protein turnover determined in this study (Spearman correlation coefficient: 0.43). (G) Distribution of protein turnover (H/Lmed) in different organelles. Abbreviations: end., endoplasmic; pl., plasma.

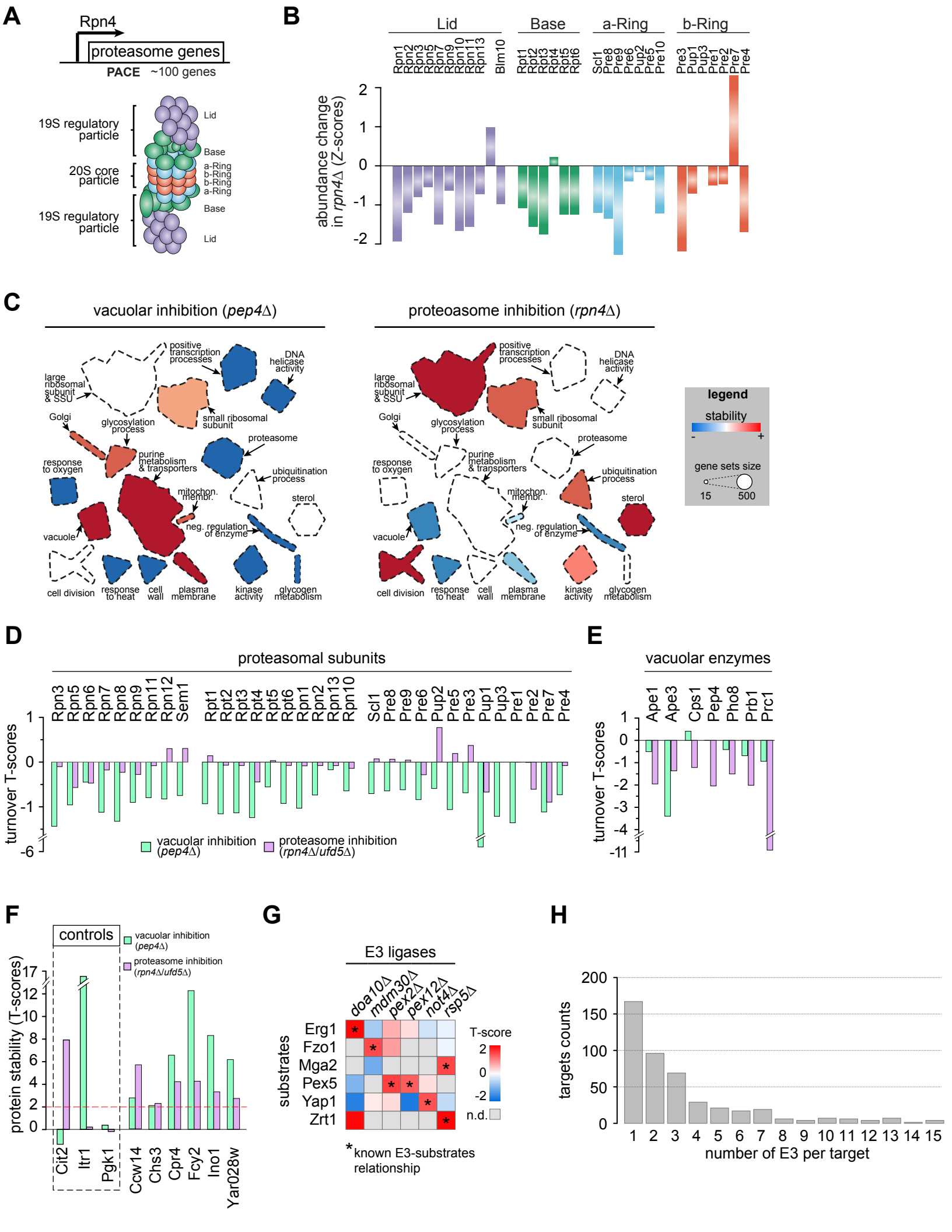
A
Rpn4
proteasome genes
PACE ~100 genes
19S regulatory particle
20S core particle
19S regulatory particle
Lid
Base
a-Ring
b-Ring
b-Ring
a-Ring
Base
Lid
B
Lid
Base
a-Ring
b-Ring
Rpn1 Rpn2 Rpn3 Rpn5 Rpn7 Rpn9 Rpn10 Rpn11 Rpn13 Blm10
Rpt1 Rpt2 Rpt3 Rpt4 Rpt5 Rpt6
Scl1 Pre8 Pre9 Pre6 Pup2 Pre5 Pre10
Pre3 Pup1 Pup3 Pre1 Pre2 Pre7 Pre4
abundance change in rpn4Δ (Z-scores)
2
1
0
-1
-2
C
vacuolar inhibition (pep4Δ)
proteoasome inhibition (rpn4Δ)
positive transcription processes
DNA helicase activity
large ribosomal subunit & SSU
small ribosomal subunit
Golgi
glycosylation process
proteasome
response to oxygen
purine metabolism & transporters
ubiquitination process
mitochon. membr.
sterol
vacuole
neg. regulation of enzyme
cell division
response to heat
cell wall
plasma membrane
kinase activity
glycogen metabolism
legend
stability
-
+
gene sets size
15
500
D
proteasomal subunits
Rpn3 Rpn5 Rpn6 Rpn7 Rpn8 Rpn9 Rpn11 Rpn12 Sem1
Rpt1 Rpt2 Rpt3 Rpt4 Rpt5 Rpt6 Rpn1 Rpn2 Rpn13 Rpn10
Scl1 Pre8 Pre9 Pre6 Pup2 Pre5 Pre3 Pup1 Pup3 Pre1 Pre2 Pre7 Pre4
turnover T-scores
1
0
-1
-6
vacuolar inhibition (pep4Δ)
proteasome inhibition (rpn4Δ/ufd5Δ)
E
vacuolar enzymes
Ape1 Ape3 Cps1 Pep4 Pho8 Prb1 Prc1
turnover T-scores
1
0
-1
-2
-3
-4
-11
F
controls
vacuolar inhibition (pep4Δ)
proteasome inhibition (rpn4Δ/ufd5Δ)
protein stability (T-scores)
17
12
10
8
6
4
2
0
Cit2 Itr1 Pgk1 Ccw14 Chs3 Cpr4 Fcy2 Ino1 Yar028w
G
E3 ligases
doa10Δ mdm30Δ pex2Δ pex12Δ not4Δ rsp5Δ
substrates
Erg1
Fzo1
Mga2
Pex5
Yap1
Zrt1
T-score
2
0
-2
n.d.
*known E3-substrates relationship
H
targets counts
200
150
100
50
0
1 2 3 4 5 6 7 8 9 10 11 12 13 14 15
number of E3 per target

Suppl. Figure 2: Coordination between Proteasomal and Vacuolar Responses, Related to Figure 2 (A) Schematic of the 26S proteasome. The 26S proteasome consists of the catalytic 20S proteasome (a barrel of four stacked rings: two outer rings and two inner rings) and the 19S regulatory particle (RP, also known as PA700). (B) Abundance fold-change of proteasome subunit in *rpn4*Δ cells. (C) Simplified version of figure 2A showing separately the effects of vacuolar and proteasomal inhibition on proteome stability. (D) Stability (T-scores) of 26S proteasome subunits in *rpn4*Δ and *pep4*Δ. (E) Stability (T-scores) of vacuolar enzymes in *rpn4*Δ and *pep4*Δ. (F) Six proteins are stabilized by impairing either proteasomal or vacuolar degradation. Itr1 is only affected by vacuolar degradation, Cit2 by proteasomal degradation, and Pgk1 is an unaffected, long-lived protein. (G) Examples of known E3 substrates identified in our T-MAP. Asterisks indicates known E3 ligase-substrate relationships. Squares are color coded by T-scores; n.d, no data. (H) Distribution of E3 effects on 457 proteins stabilized in at least one E3 ligase mutant strain.

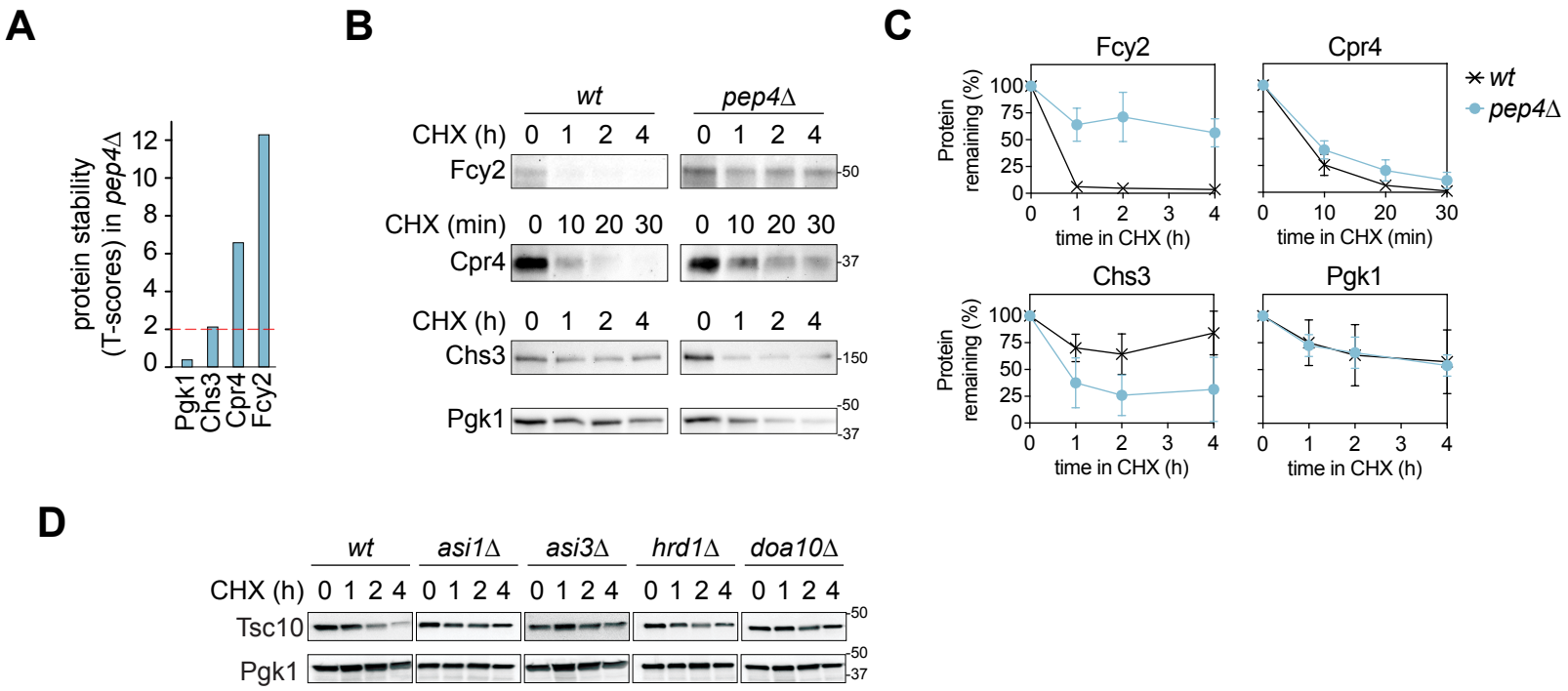

Suppl. Figure 3: Validation of Turnover Measurements Using Cycloheximide Chase Experiments, Related to Figure 2 and 4. (A) T-scores of selected proteins changes to various degrees in *pep4*Δ strain. (B) Turnover measurements of proteins in (C) after inhibition of protein synthesis using 250 µg/ml cycloheximide. Indicated genes were endogenously tagged with C-terminal 3xFLAG and proteins were detected using anti-FLAG pr anti-Pgk1 antibodies. Molecular weight marker bands indicated on the right in kDa. (C) Quantification of experiment in A from 3 independent repeats. Error bars indicate standard deviation. (D) Degradation of GFP-Tsc10 after inhibition of protein synthesis by 50 µg/ml cycloheximide in wildtype, *asi1*Δ, *asi3*Δ, *doa10*Δ, and *hrd1*Δ. Molecular weight marker bands indicated on the right in kDa.

A

Nr	Hit	Name	Probability	E-value	SS	Cols	Target Length
1	5XJY_A	ATP-binding cassette sub-family A member; membrane transporter, TRANSPORT PROTEIN; HET: NAG, BMA;{Homo sapiens}	99.42	1e-13	27.6	315	2305
2	5DO7_B	ATP-binding cassette sub-family G member; ATP-binding cassette transporter, ABCG, Sterol; 3.93A {Homo sapiens}	98.86	3.9e-10	18.3	197	685
3	5DO7_D	ATP-binding cassette sub-family G member; ATP-binding cassette transporter, ABCG, Sterol; 3.93A {Homo sapiens}	98.85	4.5e-10	18.3	197	685

B

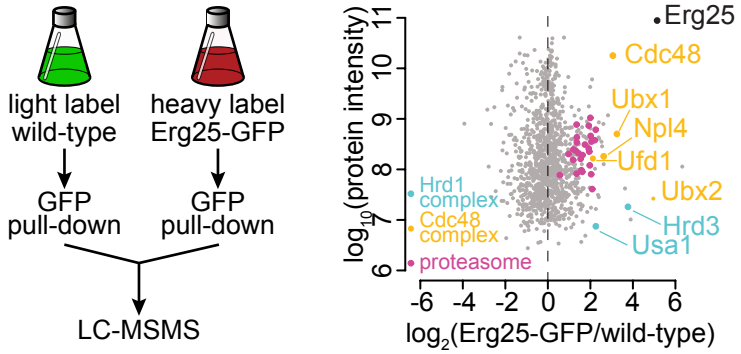

C

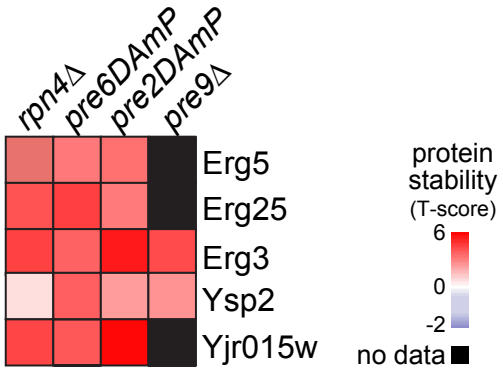

Suppl. Figure 4: Systematic Prediction of Targets for the HRD1 Branch of ERAD, Related to Figure 3. (A) HHPred alignment of *YJR015W*. (B) Erg25 physically interacts with the Hrd1 complex, Cdc48 complex, and proteasome. (left) Experimental design of SILAC-based affinity purification and MS analysis of "heavy"-labeled cells expressing GFP-tagged Erg25 and untagged control cells. (right) Protein intensities are plotted against normalized heavy/light SILAC ratios. (C) T-scores of Hrd1 targets in cells with impaired proteasomal activity deleted for either *RPN4* or *PRE9* or expressing the DAMP allele of the essential genes *PRE2* and *PRE6*. Black squares indicate no data.